Structural and Dynamic Properties of a Hydrogen Bond from the Study of the CH3Cl–HCl Complex and Isotopic Species

ARTICLE *in* THE JOURNAL OF PHYSICAL CHEMISTRY A · OCTOBER 2013

Impact Factor: 2.69 · DOI: 10.1021/jp407309a · Source: PubMed

4 AUTHORS, INCLUDING:

Pierre Asselin
Pierre and Marie Curie University - Paris 6
40 PUBLICATIONS **384** CITATIONS
SEE PROFILE

Pascale Soulard
Pierre and Marie Curie University - Paris 6
34 PUBLICATIONS **404** CITATIONS
SEE PROFILE

THE JOURNAL OF PHYSICAL CHEMISTRY A

Article

pubs.acs.org/JPCA

Structural and Dynamic Properties of a Hydrogen Bond from the Study of the CH_3Cl–HCl Complex and Isotopic Species

Manuel Goubet,*[,†] Pierre Asselin,[‡,§] Pascale Soulard,[‡,§] and Bruno Madebène[‡,§]

[†]Laboratoire de Physique des Lasers, Atomes et Molécules, UMR 8523, CNRS Université de Lille 1, F-59655 Villeneuve d'Ascq Cedex, France

[‡]Laboratoire de Dynamique, Interactions et Réactivité (LADIR), UPMC Université Paris 06, UMR 7075, F-75005 Paris, France

[§]Laboratoire de Dynamique, Interactions et Réactivité (LADIR), CNRS, UMR 7075, F-75005 Paris, France

Supporting Information

ABSTRACT: The microwave (4–20 GHz range) and infrared (HCl and DCl stretch ranges) spectra of six isotopic species of the CH_3Cl–HCl hydrogen bond complex have been recorded for the first time and analyzed with the support of high level ab initio calculations (MP2 and CCSD(T) levels). Accurate molecular parameters, including rotational, quartic centrifugal distortion, and nuclear-quadrupole coupling constants, vibrational frequencies, and anharmonic coupling constants, are presented in this paper. These parameters have then been used to estimate the hydrogen bond geometry and confirm the strong coupling between intramolecular and low frequency intermolecular modes. Experimental and theoretical evidence, in agreement with each other, tend to point out a free rotation of the CH_3Cl unit in the complex, emphasizing the very peculiar dynamical properties of a hydrogen bond and, consequently, the necessity of taking those effects into account to correctly model the intra- and intermolecular interactions.

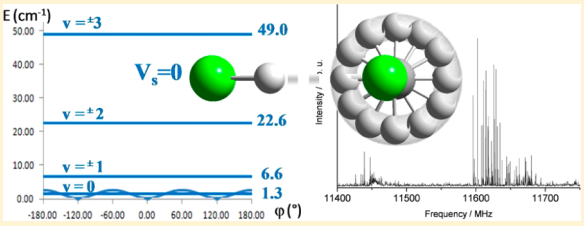

I. INTRODUCTION

The importance of hydrogen bonding is nowadays well established in many areas of physical-chemistry and biology such as phase transitions and condensed matter,[1] nuclear physics,[2] chemical reaction pathways,[3,4] planetary atmospheres,[5] secondary structures in biomolecules[6] or molecular recognition,[7] nonexhaustively. The structural (e.g., nonlinearity) and dynamical (e.g., strong vibrational couplings) properties of a hydrogen bond impose different treatments than for "conventional" chemical bonds.[8] To quantify such properties, combined experimental and theoretical studies have become a standard. In particular, spectroscopic observations of gas phase samples isolated in a supersonic expansion provide experimental data directly comparable to ab initio calculations by avoiding thermal excitation and environmental effects.[9] Once confidence in the theoretical approach is established, the resulting hydrogen bond characteristics can be used in, or to calibrate against them, the molecular mechanics models.[10,11]

As complexity grows with the size of the system, explorative studies on model systems appear mandatory. Complexes involving di- or triatomic molecules have been extensively studied using various experimental techniques,[12] unraveling their structural anisotropy and vibrational dynamic associated with strong anharmonic couplings.[13−17] In some cases, taking into account experimental results as references made possible the construction of highly accurate potential energy surfaces.[18,19] When a bigger unit is involved, such as an organic base, the vibrational analysis becomes more challenging due to homogeneous (predissociation and/or intramolecular vibrational redistribution)[20] and inhomogeneous (hot band sequences) broadening effects.[21] For a long time, studies have been limited to rotational spectroscopy[22,23] and cryogenic matrices[24−26] until the use of supersonic jets coupled to broadband Fourier transform infrared (FTIR) spectrometers, which brought enough spectral simplification to understand the confused pattern of static cell spectra.[27,28] Thanks to the recent works on several medium to high strength hydrogen bond complexes, the strong anharmonic couplings scheme between inter- and intramolecular vibrational modes is now well established.[29] A very complete review on hydrogen bond clusters probed by broadband FTIR spectroscopy synchronized to a series of high-throughput supersonic nozzle approaches has recently been published by Suhm et al.[30]

In between remains a lack of data on weakly bonded systems involving relatively large monomers. As more complexity should arise from an increased flexibility associated with a still relatively large number of degrees of freedom, the continuity between small van der Waals complexes and strongly hydrogen bonded systems is not straightforward. Therefore, complexes with a halogen atom as proton acceptor are obvious prototypes of such a class. In this realm, a combined study of the CH_3Cl–HCl complex and its isotopologues has been performed using Fourier transform microwave (FTMW) spectroscopy, cooled static cell and

Received: July 23, 2013
Revised: October 2, 2013

   dx.doi.org/10.1021/jp407309a | J. Phys. Chem. A XXXX, XXX, XXX–XXX

supersonic jet FTIR spectroscopy with the continuous support of high level ab initio calculations. After a brief review of the experimental setups, experimental and theoretical results will be presented. Then, the peculiar structural and dynamical properties of this hydrogen bond complex will be discussed.

II. EXPERIMENTAL SECTION

Products. Gaseous Chloromethane (99.5+ %), chloromethane-d_3 (99.5% atom D,) and hydrogen chloride (>99%) were purchased from Air Liquide, Sigma-Aldrich, and Messer-Griesheim and used without any further purification. Deuterium chloride was synthesized by reaction of PCl_5 with D_2O (Euriso Top 99.9% atom D).

FTMW Spectroscopy Experiment. Rotational spectra were recorded in the 4−20 GHz frequency range using the pulsed supersonic jet FTMW spectrometer of the PhLAM Laboratory in Lille.[31] The two partners were mixed in a Teflon coated stainless steel cylinder to achieve a dilution of about 5% in 2500 hPa of neon. The mixture was introduced into a Fabry−Perot cavity through a conventional series 9 General Valve pinhole nozzle (0.8 mm) at a repetition rate of 1.5 Hz. Complexes were polarized within the supersonic expansion by a 2 μs pulse and the free-induction decay signal was detected and digitized into 4096 channels. After transformation of the time domain signal, lines were observed as Doppler doublets. Transition frequencies were measured as an average frequency of the two Doppler components and for most of the lines the uncertainty of the measurement is estimated to be 2.4 kHz.

FTIR Spectroscopy Experiments. The LADIR laboratory's supersonic jet-FTIR spectrometer device has been described in detail elsewhere.[32] Briefly, a gas premixture of 10−20% of CH_3Cl seeded in argon was meeting neat HCl far upstream from the collision zone. The HCl/CH_3Cl/Ar ternary mixture was expanded at a stagnation pressure P_0 of about 120 hPa through a pinhole nozzle of 0.74 mm of diameter. To increase the production of complexes, the gas mixture was precooled to about 220 K upstream from the nozzle. The temperature regulation was obtained by combining the cooling of a stainless steel double-wall hose cylinder containing liquid nitrogen and the heating of an ohmic resistance, both fitted to the nozzle. Hydrogen bonded complexes obtained from CH_3Cl and HCl were finally probed by the 16-pass arrangement of a tungsten filament lamp issued from the Bruker IFS 120 HR interferometer and focused on a InSb detector equipped with a band-pass filter centered around the HCl (2750−2800 cm^{-1}) or DCl (2000−2050 cm^{-1}) stretching region. Each spectrum is the Fourier transform of 600 and 700 coadded interferograms recorded at 0.2 and 0.1 cm^{-1} resolution, respectively. The use of a resolution better than 0.2 cm^{-1} for CH_3Cl−HCl practically did not reduce the width of the observed rotational lines which gives upper limits for the effective homogeneous line width γ.

Cell experiments were performed at 0.1 cm^{-1} resolution with the 85 cm thermally regulated cell already described in previous studies.[27,33] The small binding energy of the CH_3Cl−HCl dimer (calculated to about 953 cm^{-1}; see hereafter) required the use of relatively low temperatures and equilibrium pressures of some tens of hectopascals to detect a significant absorption signal. Fortunately, the low boiling point of both components (182 and 158 K for CH_3Cl and HCl, respectively) enabled us to stabilize a significant density of dimers around 200 K in static cell conditions without condensation.

III. THEORETICAL CALCULATIONS

Second order Møller−Plesset calculations (MP2) were carried out using the Gaussian09 software package.[34] Coupled clusters (CCSD(T)) calculations were carried out using the Molpro2010 package.[35] The frozen-core approximation was used throughout. Dunning and co-workers[36−38] augmented correlation consistent basis set aug-cc-pVXZ (X = D, T, Q) were used (denoted hereafter AVDZ, AVTZ, and AVQZ). All geometries optimizations were performed using "tight" convergence criteria. Extrapolations to complete basis set (CBS) for energies, structural parameters, and frequencies were performed from AVDZ, AVTZ, and AVQZ results using eq 1.[39,40]

$$E_X = E_{CBS} + \alpha \exp(-(X-1)) + \beta \exp(-(X-1)^2) \qquad X = 2, 3, 4 \tag{1}$$

All calculations were only performed for the ^{35}Cl isotope. At the MP2 level, anharmonic frequencies were calculated using the second-order vibrational perturbation theory (VPT2) as implemented in Gaussian09.[41] Anharmonic correction have been extrapolated to the CCSD(T) level using eq 2 where ω and υ are the harmonic and anharmonic frequencies, respectively.

$$\upsilon_{CCSD(T)} = \omega_{CCSD(T)} - (\omega_{MP2} - \upsilon_{MP2}) \tag{2}$$

The one-dimensional cuts of the total potential energy surface (1D PES) were analyzed by solving the one-dimensional vibrational Schrödinger equation with a home-made program based on a Fourier grid Hamiltonian,[42,43] which provides eigenvalues and eigenfunctions for a periodic or aperiodic discrete PES.

IV. RESULTS AND ANALYSIS

FTMW Spectroscopy. Pure rotation spectra recorded using the FTMW spectrometer exhibited rotational lines with a nuclear-quadrupole hyperfine structure, due to the two chlorine atoms (I = 3/2), spreading over up to about 30 MHz. ^{37}Cl isotopic species were observed in natural abundance so that the sample was composed of 56% of $CH_3{}^{35}Cl$−$H^{35}Cl$, 19% of $CH_3{}^{35}Cl$−$H^{37}Cl$ and $CH_3{}^{37}Cl$−$H^{35}Cl$, and 6% of $CH_3{}^{37}Cl$−$H^{37}Cl$. A part of the low resolution (300 kHz) spectrum is displayed in Figure 1a and an example of high resolution (2.4 kHz) recorded lines is displayed in Figure 1b. For the deuterated species (CD_3Cl−HCl and CH_3Cl−DCl), no attempt was made to analyze the spectra of complexes containing ^{37}Cl atom(s) because such multiple isotopic substitutions are not relevant for the determination of the geometry.[44] The predictions and fits of the spectra were undertaken using the SPCAT/SPFIT programs suite.[45] The Hamiltonian used for treating the spectrum was a standard asymmetric-top Watson's S-reduction Hamiltonian in I^r representation. The hyperfine structure was modeled with the χ_{ii} (i = a, b or c) diagonal components of the nuclear-quadrupole coupling tensor of each chlorine atom, taking into account that $\chi_{aa} + \chi_{bb} + \chi_{cc} = 0$.[46] A I_{tot} coupling scheme was used: the spin I_1 of one nucleus (here Cl of HCl) couples to J to form $F_1 = I_1 + J$, which couples to the vector sum I_{tot} of the two equivalent spins (the two Cl atoms) to form $F = F_1 + I_{tot}$.[46] The initial guess for the main isotope spectrum was estimated from the ab initio set of rotational and quartic centrifugal distortion constants. The initial values of the nuclear-quadrupole coupling constants were calculated from the eQq values of

dx.doi.org/10.1021/jp407309a | J. Phys. Chem. A XXXX, XXX, XXX−XXX

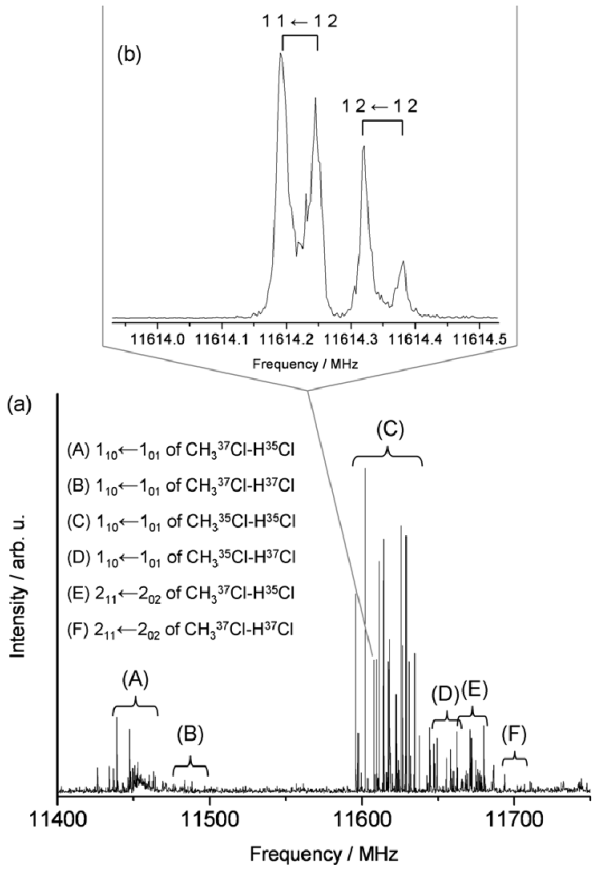

Figure 1. (a) Part of the low resolution (300 kHz) FTMW spectrum of the CH_3Cl–HCl complex in the 11 400–11 750 MHz region (attributions are in the format $J'_{K_a'K_c'} \leftarrow J''_{K_a''K_c''}$). (b) An example of recorded lines at high resolution (2.4 kHz). (Attributions of the Doppler doublets are in the format $I_{tot}'F' \leftarrow I_{tot}''F''$.)

CH_3Cl[47] and HCl[48] projected on the principal inertial axes of the complex using its ab initio equilibrium geometry. The dipole moment components were determined using the calculated Mulliken atomic charges and the Cartesian coordinates of the atoms in the principal inertial axes orientation from the MP2/AVQZ calculation, leading to values of μ_a = 1.47 D and μ_b = 2.49 D. From this reasonably predictive simulation of the spectrum ($\nu_{obs} - \nu_{calc} \sim \pm 150$ MHz for $J \leq 2$), quantum numbers were assigned to the experimental frequencies of the most intense [a]R-type and [b]R-type transitions with low values of J and F. Then, stepwise refinements of the fits were made, including levels with higher quantum numbers values and [b]Q-type transitions. The resulting molecular parameters of the $CH_3{}^{35}Cl$–$H^{35}Cl$ complex were then used to predict the spectra of the other isotopic species. Pseudotheoretical rotational constants taking into account the atomic mass changes were calculated from the ab initio molecular geometry of the main isotope. These constants were multiplied by the ratio of the corresponding experimental over theoretical constants of the main isotopic species to give pseudoexperimental constants used as initial values. Experimental quartic centrifugal distortion and nuclear-quadrupole coupling constants were introduced without any modifications. This method resulted in predictive initial spectral simulations ($\nu_{obs} - \nu_{calc}$ of only few megahertz). Rotational line assignments, measured frequencies, experimental uncertainties, and deviations from the final fits for the six studied isotopes are given in the Supporting Information. The molecular parameters obtained as the results of the fits are listed in the Table 1. Due to the lack of transitions involving high J and K values, the Δ_K and δ_2 constants remained undefined parameters. They were fixed to the ab initio values, as the fit control parameters are slightly better than when they were fixed to zero. The consistency between fitted and experimental spectra over all analyzed isotopic species gives confidence in the obtained sets of molecular constants, which is confirmed by their good agreement with the ab initio values. The very similar values of the inertial defect Δ obtained upon substitutions of in-plane atoms also tend to validate the results of the fits.

FTIR Spectroscopy. Figure 2 displays three FTIR spectra of the HCl stretching band (ν_s) of the CH_3Cl–HCl complex recorded in the static cooled cell at 196 K at 0.1 cm^{-1} resolution (a) and in the supersonic jet at 0.2 cm^{-1} resolution for two different dilutions of the HCl/CH_3Cl/Ar mixture such that rovibrational temperatures are expected to decrease from (b) to (c). Figure 3 displays our best jet-FTIR spectrum of the ν_s band of the CH_3Cl–DCl complex recorded at 0.2 cm^{-1} of resolution in the same conditions of dilution as for the coolest jet spectrum with HCl.

With respect to previously recorded cell-FTIR spectra of rigid cyclic bases bonded to strong proton donors,[49,50] the 196 K ν_s cell spectrum (Figure 2a) is almost unstructured. The characteristic pattern of resolved hot band sequences, resulting from significant anharmonic couplings between ν_s and low frequency intermolecular modes (ν_{inter}), is strongly blurred in the case of this complex. The possible scenarios of vibrational dynamics which could explain such a spectral congestion are presented hereafter in the Discussion section.

Compared to the 196 K cell spectrum, a huge simplification is observed with the supersonic jet technique. The conditions of dilution of the ternary mixture and the stagnation pressure P_0 have been adjusted to enhance the formation of the 1:1 complex with respect to larger multimers. Both jet-FTIR spectra (Figures 2b/c and 3) display one main band centered around 2790 cm^{-1} for bonded HCl and 2020 cm^{-1} for bonded DCl. Its P-, Q- and R-branch structure is characterized by a slight asymmetry on the P-branch side and an expected doublet due to the presence of the two ^{37}Cl isotopes in natural abundance. The separation in frequency between the two isotopic species is given by $\Delta\nu_{35-37} = (1 - (\mu_{35}/\mu_{37}))\nu_{35}$, where μ_i represents the reduced mass of the ^{i}Cl isotope and ν_{35} is the band center of the parent isotope. In the present case, the experimental frequency shifts (2.07(10) cm^{-1} for HCl and 2.90(20) cm^{-1} for DCl) are very close to the theoretical values (2.09 cm^{-1} for HCl and 3.06 cm^{-1} for DCl) and result in an overlap of the R-branch of the H(D)^{37}Cl component with the P-branch of the H(D)^{35}Cl one. On these grounds, both bands observed respectively at 2787.5 and 2019.6 cm^{-1} in the jet-cooled spectra of CH_3Cl–HCl and CH_3Cl–DCl are unambiguously assigned to the H–Cl and D–Cl stretching modes ν_s. The red shift relative to the monomer band center is 97.6 cm^{-1} for HCl and 71.2 cm^{-1} for DCl, which corresponds to a 3.5% frequency decrease and indicates a weak hydrogen bonding.

Ab Initio Calculations. The theoretical part of this study was carried out with a double objective. First, a reliable initial geometry is needed for the extraction of structural parameters from the experimental rotational constants. Indeed, as some coordinates have to be frozen to their ab initio values (see the Discussion section hereafter), these ones must be as realistic as

dx.doi.org/10.1021/jp407309a | J. Phys. Chem. A XXXX, XXX, XXX–XXX

Table 1. Spectroscopic Constants for the Six Studied Isotopic Species of the CH_3Cl–HCl Complex

	$CH_3{}^{35}Cl$–$H^{35}Cl$	$CH_3{}^{37}Cl$–$H^{35}Cl$	$CH_3{}^{35}Cl$–$H^{37}Cl$	$CH_3{}^{37}Cl$–$H^{37}Cl$	$CD_3{}^{35}Cl$–$H^{35}Cl$	$CH_3{}^{35}Cl$–$D^{35}Cl$
A/MHz	13251.5406(16) 13167.276[a]	13047.3398(20)	13250.7343(13)	13046.6101(19)	10837.3957(27)	13158.9545(13)
B/MHz	1863.2787(12) 1864.491[a]	1834.1941(23)	1805.1346(16)	1776.0330(21)	1808.1853(19)	1860.99979(80)
C/MHz	1629.23338(78) 1650.706[a]	1603.8629(10)	1584.59789(83)	1559.21030(91)	1552.1387(12)	1626.22524(51)
Δ_J/kHz	4.232(40) 2.57[b]	4.079(78)	3.891(51)	3.683(74)	4.577(40)	3.793(11)
Δ_{JK}/kHz	71.89(26) 76.37[b]	71.32(33)	68.04(26)	67.45(35)	58.91(27)	68.35(11)
Δ_K/kHz	793.713[b,c]	793.713[c]	793.713[c]	793.713[c]	793.713[c]	793.713[c]
δ_1/kHz	1.079(35) −0.211[b]	1.060(44)	0.837(34)	0.844(42)	1.051(32)	0.5815(86)
δ_2/kHz	−0.0667[b,c]	−0.0667[c]	−0.0667[c]	−0.0667[c]	−0.0667[c]	−0.0667[c]
χ_{aa}(HCl)/MHz	−39.2181(77) −42.122[b]	−39.659(10)	−30.9137(88)	−31.275(11)	−37.011(19)	−41.2687(90)
χ_{bb}(HCl) /MHz	11.664(11) 14.220[b]	12.099(13)	9.227(11)	9.553(17)	9.525(25)	12.568(14)
χ_{aa}(CH_3Cl)/MHz	33.5695(71) 30.162[b]	26.493(10)	33.5676(86)	26.492(10)	33.263(20)	33.3903(92)
χ_{bb}(CH_3Cl)/MHz	−71.5866(69) −65.365[b]	−56.4489(96)	−71.5794(58)	−56.4451(94)	−71.201(15)	−71.4642(96)
no. of lines	150	103	89	57	97	136
σ[d]/kHz	7.9	8.6	6.2	5.6	14.2	8.9
Δ[e]/u Å^2	0.8262	0.8352	0.8251	0.8339	−0.5265	0.7995

[a]Ab initio values of the ground state calculated at the CCSD(T)/CBS level (see text). [b]Ab initio values calculated at the MP2/AVQZ level (see text). [c]Fixed to the ab initio value of the parent molecule. [d]Microwave RMS of the fits. [e]Inertial defect $\Delta = I_c - I_a - I_b$.

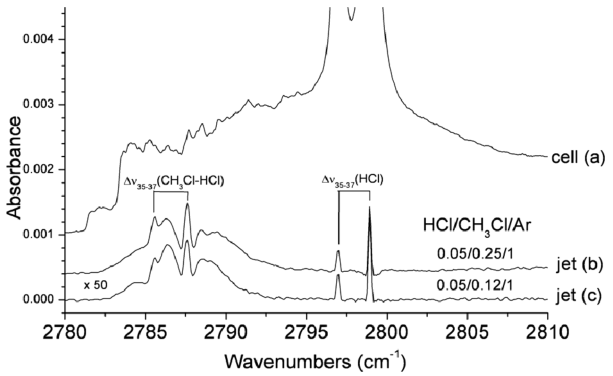

Figure 2. FTIR spectra of the HCl/CH_3Cl gas mixture recorded in the HCl stretching region of CH_3Cl–HCl: (a) in cell at 196 K; (b) and (c) in a Ar seeded jet at different dilutions.

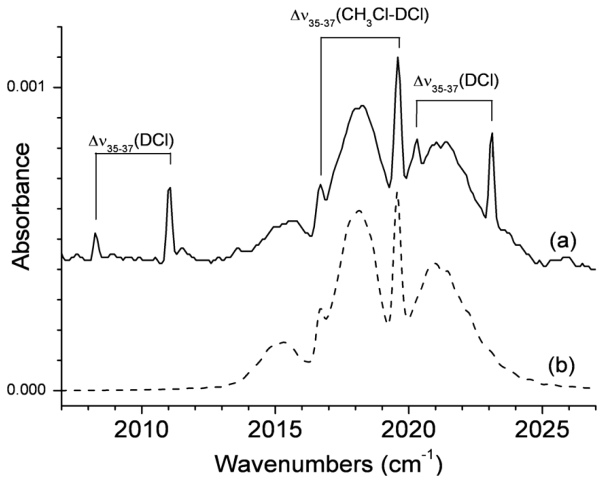

Figure 3. (a) Jet-FTIR spectrum of the υ_s band of CH_3Cl–DCl recorded at 0.1 cm^{-1} resolution. (b) Our best simulation at T_{rot} = 15 K. (Simulation parameters: υ_s = 2019.55 cm^{-1} (^{35}Cl), υ_s = 2016.65 cm^{-1} (^{37}Cl), α_A = 0 cm^{-1}, $\alpha_B + \alpha_C$ = −0.0015 cm^{-1}, γ = 0.1 cm^{-1}).

possible. Because the experimental data are observed in the vibrational ground state, the ab initio structural parameters should take into account the anharmonicity correction on the equilibrium geometry. Second, the theoretical data should reproduce as well as possible the characteristic vibrational parameters of this complex such as frequencies, red shift with respect to the free monomer, and hot band progressions involved in the stretching mode of the acid. This is necessary to guide the band assignments and to provide the parameters that could not be experimentally determined. Thus, calculations at the anharmonic level are mandatory to achieve those objectives, especially in the case of hydrogen bond complexes. In this realm, and owing to the long-range interactions between the two monomers, we opted for MP2 and CCSD(T) calculations with a large basis set (AVQZ). The effect of extrapolation to CBS has also been checked for MP2 and CCSD(T).

CH_3Cl and HCl Monomers. As a preliminary work, the methods employed here have been tested on the monomers for which accurate experimental data are available.[51,52] Structural parameters and frequencies are reported in Tables 2 and 3, respectively. The ground state structural parameters and anharmonic frequencies of CH_3Cl have been computed using the VPT2 approach at the MP2 level. The anharmonic corrections on structural parameters and frequencies obtained with MP2 have been extrapolated to provide ground state

dx.doi.org/10.1021/jp407309a | J. Phys. Chem. A XXXX, XXX, XXX–XXX

Table 2. Equilibrium and Ground State (Square Brackets) Structural Parameters of CH_3Cl and HCl Monomers (M) and the Complex (C)[a]

			MP2			CCSD(T)			exp[e]	
			AVQZ		CBS	AVQZ	CBS			
CH_3Cl param	r_{C-H}	M	108.3	[109.2][b]	108.2	108.5	108.5	[109.5][c]	*108.5*	*[109.0]*
		C (H_a)	108.3		108.3	108.6	108.6			
		C (H_b)	108.2		108.2	108.5	108.4			
	r_{C-Cl}	M	177.5	[178.3][b]	177.2	178.6	178.2	[179.0][c]	*177.6*	*[178.5]*
		C	178.1		177.7	179.2	178.8			
	a_{Cl-C-H}	M	108.5	[108.5][b]	108.5	108.3	108.4	[108.4][c]	*108.6*	*[108.6]*
		C (H_a)	108.1		108.2	108.1	108.2			
		C (H_b)	108.1		108.1	107.9	108.0			
	$d_{H-C-Cl-H}$	M	120.0	[120.0][b]	120.0	120.0	120.0	[120.0][c]	*120.0*	*[120.0]*
		C	120.0		120.0	120.1	120.1			
HCl param	r_{H-Cl}	M	127.3	[128.9][d]	127.3	127.8	127.7	[129.3][d]	*127.5*	*[128.4]*
		C	128.4		128.4	128.6	128.6	[130.4][f]		*[131.5]*
intermol param	$r_{Cl\cdots H}$		233.2		233.2	239.7	240.1	[242.5][f]		*[243.4]*
	$a_{Cl-H\cdots Cl}$		159.1		159.0	157.0	156.4	[152.6][f]		*[152.8]*
	$a_{C-Cl\cdots H}$		89.6		89.7	89.9	90.1	[91.9][f]		*[91.7]*
rot. const	A_e [A_0]	CH_3Cl	5.287	[5.196][b]	5.296	5.252	5.261	[5.169][c]	*5.268*	*[5.205]*
	B_e [B_0]	CH_3Cl	0.4482	[0.4438][b]	0.4496	0.4434	0.4450	[0.4407][c]	*0.4474*	*[0.4434]*
	B_e [B_0]	HCl	10.61	[10.36][d]	10.62	10.54	10.55	[10.29][d]	*10.59*	*[10.44]*
	A_e [A_0]	C	0.4436		0.4451	0.4384	0.4399	[0.4392][g]		*[0.4420]*
	B_e [B_0]	C	0.06489		0.06477	0.06292	0.06289	[0.06221][g]		*[0.06215]*
	C_e [C_0]	C	0.05722		0.05715	0.05561	0.05561	[0.05506][g]		*[0.05434]*

[a]Distances are in pm, angles are in degrees, and rotational constants are in cm^{-1}. [b]Ground state correction from VPT2 calculations. [c]Ground state correction extrapolated from VPT2 correction at the MP2 level (see text). [d]Ground state average value computed from the 1D-PES cut. [e]From refs 55 and 56 for CH_3Cl, from ref 52 for HCl, and from this work for the complex. [f]Ground state parameters from 1D-PES cuts (see text). [g]Computed from equilibrium parameters for CH_3Cl and ground state parameters for intermolecular values and HCl.

Table 3. Harmonic and Anharmonic (Square Brackets) Frequencies (cm^{-1}) of CH_3Cl and HCl Monomers and the Complex[a]

		MP2		CCSD(T)[b]		
		AVQZ	CBS	AVQZ	CBS	exp[c]
CH_3Cl	υ_4	3227 [3086]	3230 [3087]	3183 [3042]	3186 [3043]	*3183 [3039]*
	υ_1	3113 [3031]	3114 [3027]	3079 [2996]	3080 [2992]	*3088 [2968]*
	υ_5	1506 [1474]	1502 [1474]	1495 [1462]	1490 [1462]	*1496 [1452]*
	υ_2	1397 [1364]	1393 [1361]	1386 [1353]	1382 [1351]	*1396 [1355]*
	υ_6	1046 [1028]	1043 [1027]	1035 [1017]	1032 [1016]	*1037 [1018]*
	υ_3	770 [755]	774 [759]	745 [730]	750 [735]	*751 [733]*
HCl	υ_s	3041 [2943][d]	3038 [2942][d]	2990 [2885][d]	2988 [2886][d]	*2991 [2885]*
RMSE[e]		28 [38]	28 [37]	6 [12]	7 [10]	
CH_3Cl–HCl	υ_4	3235 [3093] (0.7)	3238 [3095]	3191 [3050]	3194 [3051]	
		3228 [3089] (0.1)	3230 [3091]	3186 [3047]	3189 [3048]	
	υ_1	3113 [3025] (15.7)	3114 [3015]	3080 [2991]	3080 [2982]	
	υ_5	1505 [1469] (4.5)	1500 [1463]	1494 [1458]	1488 [1451]	
		1505 [1458] (4.2)	1500 [1446]	1493 [1447]	1488 [1434]	
	υ_2	1399 [1364] (6.1)	1394 [1360]	1388 [1353]	1385 [1350]	
	υ_6	1056 [1031] (3.3)	1053 [1027]	1045 [1020]	1042 [1016]	
		1048 [1027] (1.6)	1045 [1023]	1037 [1015]	1034 [1012]	
	υ_3	758 [742] (23.4)	761 [745]	733 [718]	738 [722]	
	υ_s	2889 [2800] (412.6)	2884 [2797]	2879 [2790]	2875 [2788]	*[2787.5]*
	υ_{l1}	389 [311] (45.8)	388 [305]	358 [280]	353 [270]	
	υ_{l2}	294 [259] (15.4)	289 [256]	270 [236]	262 [229]	
	υ_σ	115 [99] (10.9)	115 [96]	106 [90]	105 [86]	
	$\upsilon_{\delta 1}$	77 [50] (5.5)	78 [50]	73 [45]	71 [43]	

[a]Intensities at the harmonic level (in km/mol) are reported in parentheses for the complex. [b]Anharmonic frequencies extrapolated from the MP2 anharmonic correction (see text). [c]From ref 51. for CH_3Cl, ref 52. for HCl and this work for the complex. [d]Anharmonic frequency computed from the 1D-PES cut. [e]Root Mean Squared Error from experimental frequencies.

dx.doi.org/10.1021/jp407309a | J. Phys. Chem. A XXXX, XXX, XXX–XXX

parameters and anharmonic frequencies at the CCSD(T)/CBS level (eq 2). As the implementation of the VPT2 is not available for a diatomic molecule, the HCl anharmonic frequency has been computed by solving the vibrational Schrödinger equation from MP2/AVQZ and CCSD(T)/CBS 1D-PES. The corresponding ground state vibrational wave functions Ψ_0 have been used to evaluate the average value of the acid length such as

$$\langle r_{H-Cl}\rangle_0 = \langle \Psi_0 | r_{H-Cl} | \Psi_0 \rangle$$

All theoretical methods used here correctly reproduce the structural parameters of CH_3Cl with a maximum deviation of 0.7% compared to the experimental data (Table 2). MP2/AVQZ reproduces well equilibrium and ground state parameters, in part by error compensation on the C−H bond length. However, it is well-known that MP2 overestimates the strength of hydrogen bond complexes and will not provide accurate parameters for the complex. Conversely, all CCSD(T) approaches well reproduce experimental equilibrium parameters excepted for the C−Cl distance, which is overestimated at the CCSD(T)/AVQZ level. The CBS extrapolation partially corrects this. The estimation of CCSD(T)/CBS ground state parameters from the MP2 anharmonic correction overestimates bond lengths, but their values and the corresponding A_0 and B_0 are satisfactory as their discrepancies are less than 0.7%. For the HCl molecule, all methods correctly reproduce the equilibrium length but the ground state correction is overestimated. MP2/AVQZ takes advantage of an error compensation (the slight underestimation of the equilibrium distance compensates a part of the overestimation of the anharmonic correction) to give a ground state H−Cl length in better agreement with the experiment (128.9 pm vs 128.4 pm) than the CCSD(T)/CBS one (129.3 pm).

The study of harmonic frequencies of both molecules revealed that MP2 overestimates all frequencies, with a root mean squared error (RMSE) of 28 cm^{-1} with respect to the experiment (Table 3). The stretching modes involving hydrogen atoms are the worst reproduced with an overestimation of +50 cm^{-1} for the H−Cl stretching mode and +44 cm^{-1} for the υ_4 mode of CH_3Cl. Increasing the correlation treatment to a coupled cluster level significantly improves the prediction of the harmonic frequencies. RMSE falls down to only 6−7 cm^{-1} with a maximum deviation of 10−14 cm^{-1}. For the anharmonic frequencies, the approximation consisting in adding the MP2 anharmonic correction to CCSD(T) harmonic frequencies (eq 2) provides very reliable values. Except for the υ_1 mode of CH_3Cl (symmetric C−H stretching), which is overestimated of about 30 cm^{-1} due to an underestimation of the anharmonic correction by VPT2, all other computed frequencies are only shifted by few cm^{-1} from observed frequencies. The CBS extrapolation does not bring any significant improvement on frequencies compared to CCSD(T)/AVQZ which is amply sufficient for the monomers.

CH_3Cl–HCl Complex. As mentioned in previous studies performed at lower levels (HF/6-31G**,[53] MP2/6-31+G**[54]), the complex is in the C_s point group (Figure 4). All atoms are in the symmetry plane (*ab* plane) except for two hydrogen atoms of the methyl group, denoted hereafter H_b (the in-plane atom being denoted H_a), which lie on opposite sides of the plane.

The structural parameters are reported in Table 2 together with the monomers' values. The comparison between the structural parameters of the complex and the isolated units shows that the CH_3Cl unit is almost unmodified by the formation of the complex. Very small geometry changes are induced by the hydrogen bond whatever the method used: r_{C-Cl} is slightly increased (+0.6 pm), most probably due to the implication of the chlorine atom in the hydrogen bond; consequently, the Cl−C−H angle is slightly reduced (−0.4°); the C−H distances are nearly unaffected although tiny differences between the parameters related to H_a and H_b are observed, but such small variations are difficult to interpret. As expected with the formation of a hydrogen bond, the H−Cl bond is elongated in the complex (+1.1 pm with MP2 and +0.9 pm with CCSD(T)). Concerning the intermolecular parameters, the C−Cl--H angle is independent of the method (∼ 90°). The Cl--H−Cl angle slightly decreases when going from MP2 to CCSD(T) by 2−3°, increasing the nonlinearity of the hydrogen bond. The hydrogen bond length is strongly underestimated by MP2 comparing to CCSD(T) (−7 pm) and is slightly dependent on the basis set with coupled cluster methods, as it grows from 239.7 pm (AVQZ) to 240.1 pm (CBS).

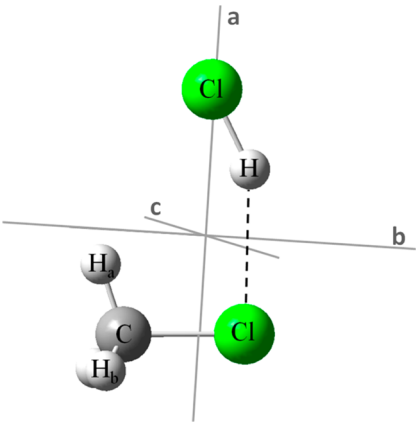

Figure 4. Calculated equilibrium structure of the CH_3Cl–HCl complex.

Experimental and theoretical frequencies of CH_3Cl, HCl, and the CH_3Cl–HCl complex are reported in Table 3. As observed for the structural parameters, the CH_3Cl unit's frequencies are nearly unaffected by the complex formation. A small splitting occurs for the degenerate modes of the free monomer (υ_4, υ_5, and υ_6). Even if the validity of such small differences is disputable, it is in agreement with the differences in the structural parameters involving H_a and H_b. The error on the H−Cl stretching mode frequency is only of 9−12 cm^{-1} with MP2 and falls down to 1−3 cm^{-1} at the CCSD(T) level. The observed red shift (97.6 cm^{-1}) is much better reproduced at the CCSD(T) level ($\Delta\upsilon_s$ = 95−98 cm^{-1}) than at the MP2 level ($\Delta\upsilon_s$ = 143−145 cm^{-1}), most probably because of the much better description of the HCl unit at the former level. For the sake of clarity, it is reminded that five intermolecular modes are appearing upon complexation: the intermolecular stretching (ν_σ); the HCl libration in-plane (ν_{l1}) and out-of-plane (ν_{l2}), which correspond here to hindered rotations of the HCl unit; the intermolecular bending in-plane ($\nu_{\delta 1}$) and out-of-plane ($\nu_{\delta 2}$), which correspond here to hindered rotations of the CH_3Cl unit. Despite the absence of direct observation of these modes in the gas phase, the calculated values of ν_{l1} and ν_{l2} can be compared to those observed for CD_3Cl–HCl in liquid argon.[53] The deuteration of the methyl group should negligibly affect the intermolecular modes (for the librations at the harmonic level, the calculated shift is lower than 1 cm^{-1}

dx.doi.org/10.1021/jp407309a | J. Phys. Chem. A XXXX, XXX, XXX−XXX

whatever the method used). A very good agreement is obtained between the observed υ_{l1} and υ_{l2} of CD_3Cl–HCl (respectively 283 and 231 cm^{-1}) and the computed librations at the CCSD(T) level for CH_3Cl–HCl (270–280 and 229–236 cm^{-1}), keeping in mind the unknown frequency shifts due to the influence of liquid argon. The $\nu_{\delta 2}$ mode is not reported in Table 3 as it cannot be described by the VPT2 calculations (indeed it resulted in a negative frequency). This peculiar mode will be discussed hereafter. However, we have assumed that the error on this mode should only affect very little the others frequencies as very low values are computed for the harmonic frequency and the vibrational coupling constants involving this mode. The very good agreement between the calculated and observed υ_s, υ_{l1}, and υ_{l2} tends to confirm this assumption.

Concerning the energetic properties, the binding energy of the complex (D_e) has been computed without counterpoise correction, the CBS value being free from basis set superposition error (BSSE). D_e is equal to 1280 and 1247 cm^{-1} at the CCSD(T)/AVQZ and CCSD(T)/CBS levels, respectively. As both D_e values are very close, this clearly shows that the BSSE is weak with the AVQZ basis set. MP2 overestimates D_e (1423 cm^{-1} with CBS), as expected for hydrogen bond complexes. The anharmonic zero point energy correction results give D_0 = 953 cm^{-1} at the CCSD(T)/CBS level, indicating that this complex is weakly bonded[57] in agreement with the small experimental red shift of the H–Cl stretching mode frequency upon complexation.

V. DISCUSSION

IR Band Contour Simulations. A homemade simulation program enabling to simulate the superposition of several band contours for an unperturbed rigid asymmetric rotor[58] is used to reproduce FTIR spectra of CH_3Cl–HCl at different rovibrational temperatures and of CH_3Cl–DCl for the coolest jet conditions. Band contour simulations are carried out in two steps.

In a first step, due to the strong rovibrational cooling within the supersonic expansion, the ν_s fundamental band is largely predominant in the jet-FTIR spectra and can be simulated to determine a first set of rovibrational and dynamic parameters. Several parameters can be fixed before starting the simulation: (i) the ground state rotational constants are accurately known from the FTMW experiments (A_0 = 0.44202 cm^{-1}, B_0 = 0.06215 cm^{-1}, and C_0 = 0.05434 cm^{-1} for CH_3Cl–HCl); (ii) the band hybridization is derived from the projection of the HCl vector onto the molecular inertial axes (85% a-type and 15% b-type for both isomers); (iii) the instrumental resolution $\Delta\nu_{fwhm}$ and the shape of the apparatus response function (Happ–Genzel) are well-known. As the band contour of the H(D)^{37}Cl isotopic species is rotationally unresolved, the band center is simulated by shifting the band center of the parent isotope of the $\Delta\nu_{35-37}$ value and taking an intensity scaling factor f_s such as $f_s(H(D)^{35}Cl)/f_s(H(D)^{37}Cl)$ = 3. Thus, the adjustable set of parameters for the jet-FTIR spectra contains the three rovibrational coupling constants α_s^X (X = A, B, C), the rotational temperature T_R in the supersonic expansion and the effective homogeneous line width γ. Figure 5 displays an expanded view of experimental jet-FTIR and synthetic spectra of CH_3Cl–HCl.

In a second step, these values are introduced in a larger set of parameters, including the contribution of anharmonic vibrational couplings to be evaluated, to reproduce as well as possible the hot band sequences observed in cell-FTIR spectra.

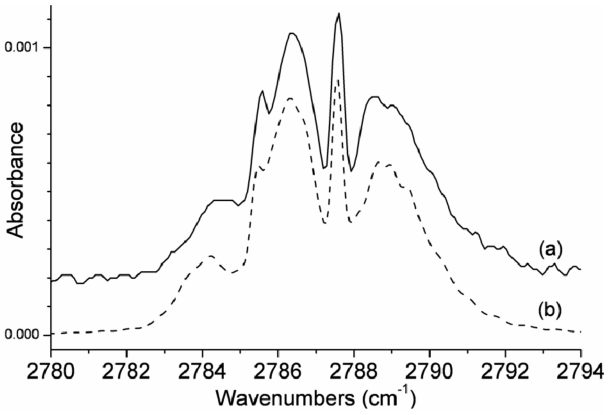

Figure 5. (a) Jet-FTIR spectrum of the υ_s band of CH_3Cl–HCl recorded at 0.2 cm^{-1} resolution. (b) Our best simulation at T_{rot} = 15 K. (Simulation parameters: υ_s = 2787.55 cm^{-1} (^{35}Cl), υ_s = 2785.41 cm^{-1} (^{37}Cl), α_A = 0 cm^{-1}, $\alpha_B + \alpha_C$ = −0.0020 cm^{-1}, γ = 0.1 cm^{-1}.)

Different scenarios have been examined by considering the strongest two-mode couplings between ν_s and the ν_{inter} (the off-diagonal elements $x_{s,inter}$ obtained from the VPT2 anharmonicity matrix) as well as the thermal occupation of the ν_{inter} calculated at the CCSD(T)/CBS anharmonic level. Figure 6 displays a comparison between the 196 K cell-FTIR spectrum and the two most probable scenarios of anharmonic couplings (denoted A and B).

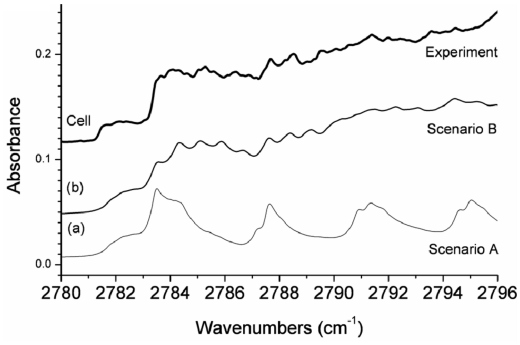

Figure 6. Comparison between the 196 K cell-FTIR spectrum of the ν_s band of CH_3Cl–HCl and the two most probable scenarios of anharmonic coupling between ν_s and intermolecular modes: (a) the scenario A refers to couplings between ν_s and all intermolecular modes apart from the intermolecular bending out-of-plane ($\nu_{\delta 2}$); (b) the scenario B includes with respect to scenario A the coupling between ν_s and $\nu_{\delta 2}$. (Simulation parameters: ν_σ = 86 cm^{-1}, $\nu_{\delta 1}$ = 43 cm^{-1}, $\nu_{\delta 2}$ = 5 cm^{-1}, $x_{s,\sigma}$ = 7.4 cm^{-1}, $x_{s,\delta 1}$ = 3.7 cm^{-1}, $x_{s,\delta 2}$ = 0.8 cm^{-1}.)

The scenario A represents the case of a multimode coupling between ν_s and all others ν_{inter} than $\nu_{\delta 2}$ (intermolecular bending out-of-plane) because no reliable frequency value could be obtained from the anharmonic vibrational calculations. In the case of CH_3Cl–HCl, ν_{l1} and ν_{l2} fall below 300 cm^{-1} and are likely to contribute to the 196 K cell spectrum. However, the magnitudes of the $x_{s,li}$ coupling constants (32 and 45 cm^{-1} for ν_{l1} and ν_{l2}, respectively) push their hot bands sequences largely outside the investigated spectral window. Sixteen hot transitions identified with the notation $|v\rangle = |v_s\ v_{\delta 1}\ v_\sigma\ v_{l1}\ v_{l2}\rangle$ have been selected for the simulation, on the grounds of relative intensities larger than 10% of the fundamental band and blue-shifted band centers according to the anharmonic expansion of

dx.doi.org/10.1021/jp407309a | J. Phys. Chem. A XXXX, XXX, XXX–XXX

the vibrational energy in the state |v⟩. The synthetic 196 K spectrum corresponding to the scenario A is reported in Figure 6a and clearly shows that the simulated ν_s profile deviates from the experimental one when $\nu_{\delta 2}$ is not considered.

Ab initio calculations, aiming at characterizing the $\nu_{\delta 2}$ mode (see discussion hereafter), indicate some trends that could explain the confused pattern of the overall ν_s band. In particular, a very low frequency is expected and the magnitude of the anharmonic coupling $x_{s,\delta 2}$ is difficult to precisely evaluate but should fall in the range 0−1 cm^{-1}. On these grounds, a tentative simulation of the ν_s band has been performed by considering all the ν_{inter} modes (scenario B) with adjustable values, in the 5−50 cm^{-1} range for the $\nu_{\delta 2}$ frequency and in the 0.1−1 cm^{-1} range for the $x_{s,\delta 2}$ constant. The much better agreement between the experimental and our best synthetic spectrum for the scenario B (Figure 6b) tends to confirm the preponderant role of this very floppy mode in the vibrational dynamics of the complex.

Intermolecular Bending Out-of-Plane Mode. At this stage, there is a strong contradiction between the use of a semirigid model to analyze the MW spectra and the introduction of a low frequency mode, arising from a floppy large amplitude motion, needed to correctly simulate the IR spectrum. Thus, each way has been more deeply investigated to understand this controversy. In one hand, the determination of an effective geometry would validate the set of rotational constants obtained from the distortable rotor model. On the other hand, explorations of the ab initio PES should shed some light on the dynamics of the $\nu_{\delta 2}$ mode.

Determination of the Substitution Structure r_s. The observation of isotopic species makes possible the determination of an effective structure from Costain's method[59] based on Kraitchman's equations.[44] In the present case, the analysis of five isotopic species gave rise to 15 experimental rotational constants to be fitted. $CH_3{}^{37}Cl-H^{37}Cl$ was excluded from the fits because it is redundant with the two monosubstituted complexes and should not improve the positioning of the two chlorine atoms.[44] The complex having a C_s symmetry, all z Cartesian coordinates, referring to the inertial axis c perpendicular to the symmetry plane (ab plane), were fixed. The ^{13}C isotope has not been observed, so the carbon atom's coordinates have to be fixed. These assumptions are leading to 12 free parameters over the 21 Cartesian coordinates. In addition, it is expected that some other coordinates will remain undefined (see hereafter), so an initial guess for the geometry as realistic as possible is needed. The VPT2 correction failed in calculating the ground state structural parameters of this complex. Indeed, the ground state length of the acid is shorter in the complex than the equilibrium length of the isolated monomer (125.8 pm vs 127.3 pm at MP2/AVQZ level), which is physically not reasonable. To provide an ab initio estimation of the ground state values of the intermolecular structural parameters and the H−Cl length, the average value of each parameter was computed from the one-dimensional vibrational wave functions in the ground state. These wave functions were obtained by solving the vibrational Schrödinger equation from one-dimensional cuts in the total CCSD(T)/CBS PES along each coordinate of interest.

1. for the H−Cl bond: variation of the H−Cl length fixing the center of mass of the acid
2. for the intermolecular bond: variation of the distance between monomers' center of mass
3. for the Cl--H−Cl angle: rotation of HCl around its center of mass in the C_s plane
4. for the C−Cl--H angle: rotation of CH_3Cl around its center of mass in the C_s plane

Such analyses along the out-of-plane coordinates (dihedral angles) are pointless due to the C_s symmetry: the PES cut would be symmetric so that the wave function would be symmetric as well, resulting in an average structural parameter identical to the equilibrium one. Finally, the CH_3Cl unit was kept to its equilibrium structure. Theoretical ground state structural parameters obtained from this approach (reported in Table 2) led to A_0, B_0, and C_0 constants for which the agreement with the experimental ones (errors of 0.6%, 0.1%, and 1.3%, respectively) was found good enough to rely on. It is noteworthy that the B and C constants have been significantly improved compared to the initial equilibrium values (errors of 1.2% and 2.3%, respectively).

A homemade program, based on a Levenberg−Marquardt least-squares refinements procedure, was developed to obtain the effective structure from the fit of the ground state rotational constants. The Cartesian coordinates of the atoms of the parent molecule are the adjustable parameters. The three rotational constants are deduced from this geometry. Then, the rotational constants of each other isotopic species are calculated after reorientation of its geometry in the principal axis system, successively. Finally, all constants are compared to the experimental values, which are the data, and so on until convergence. The standard deviations σ_i of each parameter p_i were calculated from the square root of the diagonal elements of the last covariance matrix extracted from the least-squares routine. The ab initio structure was used as an initial guess. In a first step, all 12 parameters were optimized because their number was slightly lower than the number of data (15 rotational constants). Then, the parameter having the highest standard deviation was fixed to its ab initio value, and so on until all free parameters were considered as statistically defined ($3\sigma_i < p_i$). Using this procedure, (i) the y coordinate of the Cl atom of HCl, (ii) the H atom of HCl, and (iii) the x coordinate of the H_a atom had to be fixed to their ab initio values. As a final result, the 15 experimental rotational constants are fitted with a RMS error of about 14 MHz. This too large error 3 orders of magnitude bigger than the experimental standard deviations of the constants justifies a deeper analysis of the positioning of the atoms.

Beyond the simple numerical point of view, the impossibility of defining some coordinates may be explained in terms of the molecular structure. (i) The Cl atom of HCl is almost located on the inertial axis a (Figure 4). Thus, its y coordinates, nearly equal to zero, cannot be determined as the error is inversely proportional to the parameter's value.[59] (ii) It is well-known that the present method is not strictly appropriate for an hydrogen atom because the mass change upon substitution to deuterium atom is large (about 2 times).[60] Moreover, it is the closest atom to the center of mass of the complex (Figure 4). In fact, the difficulties in positioning this H atom from a H to D substitution is due to the Ubbelohde effect.[61] However, as long as all other substituted atoms may move freely around it, particularly the two chlorine atoms, fixing these coordinates to their ab initio values should not prevent the fit from obtaining a realistic geometry of the hydrogen bond. This assumption may be verified by two more independent ways as follows.

dx.doi.org/10.1021/jp407309a | J. Phys. Chem. A XXXX, XXX, XXX−XXX

First, Costain suggested in his early paper[59] that the position of a particular atom may be obtained only by fitting the rotational constants of the parent and the corresponding monosubstituted molecules. This procedure has been applied to each substituted atom individually, by fixing all other coordinates to their values obtained from the global fit. In each case, the numerically undefined coordinates remained undefined but for the others, the resulting position was within the standard deviation estimated from the global fit. In the same realm, considering that the CH_3Cl unit is unaffected (or very little) by the complexation, its geometry has been fixed to the known fundamental state's one[55] and only the HCl unit parameters have been optimized to reproduce the rotational constants of the $CH_3Cl{-}H^{35}Cl$, $CH_3Cl{-}H^{37}Cl$, and $CH_3Cl{-}$DCl isotopes. These fittings also resulted in the same undefined coordinates and positions within the standard deviations of the global fit.

Second, the orientation of a bond involving a singly bonded terminal quadrupolar nucleus (here Cl of H−Cl) can be obtained from the nuclear-quadrupole coupling tensor components, as reviewed by Legon in ref 22. From the experimental values of the diagonal components of the nuclear-quadrupole coupling tensor, the off-diagonal component χ_{ab} = 32.5214 MHz is estimated using eq 8 of ref 22. This value introduced in eq 7 of ref 22 leads to a value of α_{az} = 26.0°, which is the angle between the principal inertial axis a and the axis of the H−Cl bond z. For comparison, a value of α_{az} = 27.0° is calculated from the ab initio geometry and a value of α_{az} = 25.3° is obtained from the Cartesian coordinates derived from the fits. These values arising from three independent sources are in sufficiently good agreement to give a good confidence in the positioning of the HCl unit even if some coordinates have to be fixed during the fitting procedures.

Concerning the CH_3Cl unit, the fact that the x coordinate of H_a cannot be defined (iii) cannot be explained by the same arguments. Indeed, even if the method is averagely appropriate for hydrogen atoms, errors on the bond lengths of the order of 0.5 pm are expected.[60] In the case of the C−H_b bonds, when the x coordinate of H_a is free, the deviation from the ab initio values goes up to −5 pm. Also, the free parameters involving H_a and H_b display the larger standard deviations (from 10 to 30%). Even if the estimation of the errors during calculation of an effective structure is a complicated issue, the standard deviations should at least lead to a reliable order of magnitude. In addition, fitting procedures with adjustable z coordinates of the H_b atoms were diverging. Moreover, the final step of the fitting procedure described here above has been repeated after a rotation of 180° of CH_3Cl around its axis (with H_a pointing away from instead of toward HCl). It has resulted in almost the same estimations of the rotational constants with the x coordinates of the H_b atoms becoming undefined. This undefined positioning of the H atoms is confirmed from the ab initio structure calculations: computations of the rotational constants over a complete rotation of CH_3Cl around its axis, freezing all other coordinates, show variations lower than 100 kHz, which is far below the fit error of about 14 MHz. This could be explained by the fact that the CH_3Cl unit is nearly unaffected by the formation of the complex: it remains a symmetric top and its rotation about its symmetry axis does not affect the mass distribution within the complex.

In the present case, the robust method of estimating a r_s structure from isotopic substitutions[60] has unexpectedly failed. The various tests performed here tend to attribute this failure to the CH_3Cl unit.

Explorations of the ab Initio PES. The VPT2 approach and the use of rectilinear normal coordinates are not able to describe a low frequency vibrational mode with several minima separated by low energy barriers, such as the $\nu_{\delta 2}$ mode. Indeed, a 3-fold potential energy curve is expected for this hindered rotation of the CH_3Cl unit, which looks like a methyl group internal rotation. Then, a variational approach has been used to estimate its frequency and evaluate its dynamical properties. Two solutions were chosen. In the first one, the vibrational Schrödinger equation was solved from the 1D cut of the PES along the $\nu_{\delta 2}$ coordinate. The second one was taking into account the coupling between $\nu_{\delta 2}$ and ν_s by exploring the 2D PES computed along both modes' coordinates using an adiabatic [1 + 1] decomposition: at selected values along the $\nu_{\delta 2}$ coordinate, a 1D cut of the PES along the ν_s coordinate was computed and the vibrational Schrödinger equation was solved. The obtained eigenvalues led to adiabatic 1D-PES cuts along the $\nu_{\delta 2}$ coordinate depending on the vibrational state of the acid stretching (v_s = 0, 1, 2, ...). By solving the vibrational Schrodinger equation for $\nu_{\delta 2}$ on these adiabatic surfaces, we obtained vibrational energies for this mode depending on a vibrationally excited state of the acid. This approach has already given suitable results on previous hydrogen bond complexes, even with tunneling effect.[62−65] To ensure the equivalence of the three minima, a C_3 symmetry has been imposed to CH_3Cl in the complex, which affects the energy by less than 2 cm^{-1}. The cuts were made by a rotation around the C−Cl axis from 0 to 60° and completed by symmetry to cover the full rotation [−180, +180°]. The PES have been computed at CCSD(T)/AVQZ and CCSD(T)/CBS level of theory. As they led to similar results, only the CBS results are reported here.

Figure 7 brings together the one-dimensional cuts obtained along the $\nu_{\delta 2}$ coordinate without couplings (bottom graphic), coupled to the acid in the ground state v_s = 0 (middle graphic) and coupled to the acid in the first excited state v_s = 1 (top graphic), and their associated vibrational energies.

Without couplings, the barrier to rotation is 36 cm^{-1}. Vibrational energy states are degenerate in pairs to v = 1 and v = 2 (denoted by ± on the figure) and a break occurs for v = 3. The evolution of energy is somewhat irregular and we found a very low frequency of 3.6 cm^{-1} for $\nu_{\delta 2}$.

When v_s = 0, the height of the barrier is strongly reduced to 3 cm^{-1}, which means that the CH_3Cl unit rotates freely and that the system behaves as a particle in a periodic box. This situation is reflected in the evolution of the calculated frequencies: we obtain 5.3, 16.0, and 26.4 cm^{-1} for the transitions 0 → 1, 1 → 2, and 2 → 3. This regular progression of the frequencies is such as X, 3X, 5X, where X is the value of the rotational constant A of the isolated CH_3Cl.[56]

When v_s = 1, the barrier slightly increases to 8 cm^{-1}. The evolution of the frequencies is almost the same (5.1, 16.5, and 26.3 cm^{-1}). The differences between frequencies obtained for v_s = 0 and v_s = 1 enable us to estimate the variations of the hot bands of υ_s, which are found to be very small (−0.2, +0.5, −0.1 cm^{-1}) and falls in the limits of the model used.

These calculations, in the case of a coupled scheme, tend to confirm the assumptions made to correctly reproduce the cell-FTIR spectrum, which are a very low frequency for the $\nu_{\delta 2}$ mode, around 5 cm^{-1}, and a very small anharmonic coupling constant between this mode and ν_s, lower than 1 cm^{-1}.

dx.doi.org/10.1021/jp407309a | J. Phys. Chem. A XXXX, XXX, XXX−XXX

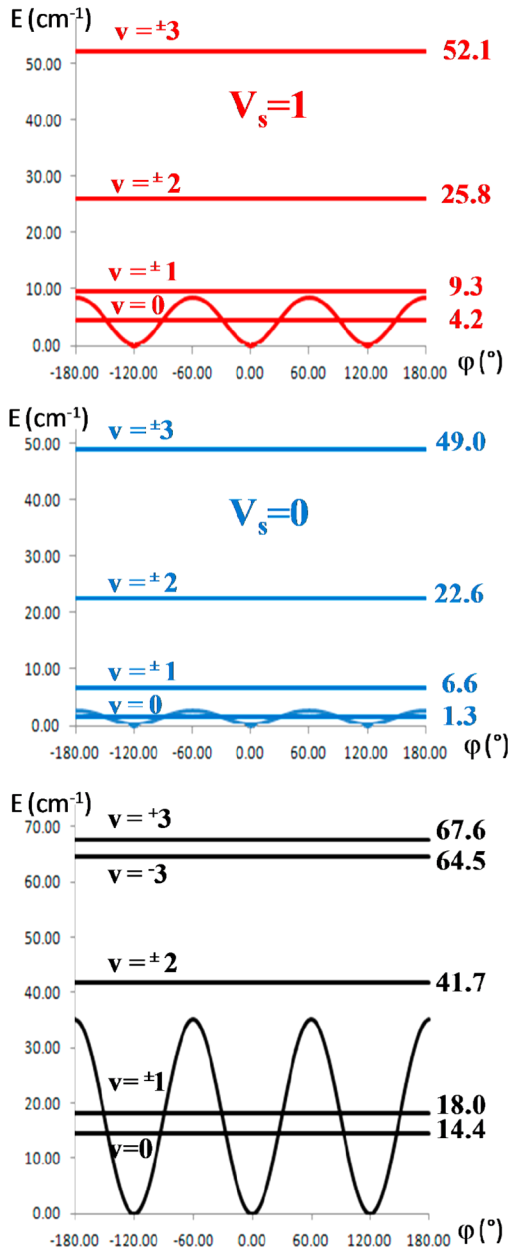

Figure 7. One-dimensional potential energy curves along the intermolecular bending out-of-plane ($\nu_{\delta 2}$) coordinate φ and associated vibrational energies: uncoupled (bottom graphic) and coupled with H−Cl stretching mode (ν_s): adiabatic surfaces for ν_s = 0 (middle graphic) and for ν_s = 1 (top graphic). Energies are in cm^{-1} and angles are in degree.

Inertial Defect. The inertial defect Δ depends on the out-of-plane atoms, which in the present case are those involved in the internal rotor. The 3-fold barrier height V_3 can be estimated from the experimental value of Δ[66] by using the equations developed by Herschbach.[67] For this purpose, the moment of inertia of the internal top about its symmetry axis I_α = 3.2396 u Å^2 is deduced from the constant A_0 of CH_3Cl.[56] Then, two sets of geometrical parameters and rigid rotor rotational constants are used for comparison: from the ab initio calculations (denoted hereafter set a) and from the calculated r_s structure (set b). The obtained Herschbach's perturbation coefficients $W_{00}^{(2)}$ are 0.636 459 for (a) and 0.625 946 for (b). These values being outside of the tabulated range,[67] values of the barrier coefficients s = 0.90 for (a) and 1.09 for (b) are calculated from a linear extrapolation of the two last tabulated values. The asymptotic character of s as a function of $W_{00}^{(2)}$ makes this approximation very reasonable. Finally, V_3 are estimated to 11 cm^{-1} for (a) and 13 cm^{-1} for (b). Both values obtained from two independent ways match well between them and qualitatively agree with the value of 3 cm^{-1} obtained from the exploration of the PES in the coupling scheme with ν_s, keeping in mind that the couplings with others vibrational modes were ignored. In addition, the dissociation energy D_e can be estimated from the constants B_{00}, C_{00}, and Δ_J and the distance between the center of mass of the two units R_{CM}.[66] The obtained values, i.e., 597 cm^{-1} for (a) and 633 cm^{-1} for (b), are underestimated with respect to the ab initio value (953 cm^{-1}), which can be explained by the fact that the axis formed by the two centers of mass is not quite parallel to the inertial axis of the complex.

The variation of the inertial defect upon H_3 to D_3 isotopic substitutions can be used to retrieve the distance between the two equivalent atoms out of the symmetry plane for a system in the C_s point group (see formula 16 of ref 59). A z coordinate for the H_b atoms of ±57.9 pm is obtained from this formula. With a C−H bond length of 109 pm (GS value in the CH_3Cl monomer),[55] this corresponds to a much too small H−C−H angle of about 64°, when a value around 110° is expected.[55]

CH_3Cl Unit's Free Rotation. Experimental and theoretical evidence, in agreement with each other, tend to point out a free rotation of the CH_3Cl unit in the complex, explaining the controversy around the $\nu_{\delta 2}$ mode. A confused pattern observed at 196 K, which strongly simplifies under jet-cooled conditions is the signature of a hot band sequence involving a very low frequency with a small anharmonic coupling constant. The presence of such a mode is supported by the ab initio calculations. When a coupling with ν_s is considered, the GS of $\nu_{\delta 2}$ is most probably falling over the barrier to internal rotation of the CH_3Cl unit estimated to about 10 cm^{-1} from both experiment and theory. The experimental inertial defect can be reproduced by introducing the internal rotation as a perturbation to the rigid rotor constants, Then, it appears obvious that the rotational spectrum is influenced by this very floppy internal motion so that the rotational constants obtained using a semirigid rotor model are effectives. When effective, their reproduction from a r_s structure is unsuccessful and several tests together with the use of the variation of the inertial defect upon H_3 to D_3 substitutions tend to locate the problem at the CH_3Cl unit. This failure may be explained by the two following considerations. First, considering that the r_s method is appropriate for rigid (or semirigid) rotors, the fit of effective constants has resulted in the estimation of the rigid rotor constants, explaining the discrepancies as large as several megahertz. This may be confirmed by their successful use to estimate the V_3 value. Second, the internal motion corresponds to a rotation of a symmetric top about its symmetry axis, which is almost parallel to the b inertial axis of the complex, so the mass distribution within the complex is unaffected by this motion. Therefore, the position of the H_b atoms can not be obtained from methods using the absolute values of the moments of inertia such as the r_s structure or the variation of the inertial defect upon H_3 to D_3 substitutions.

VI . CONCLUSION

With the support of high level ab initio calculations (CCSD(T)/CBS), we recorded and analyzed the FTMW

dx.doi.org/10.1021/jp407309a | J. Phys. Chem. A XXXX, XXX, XXX−XXX

spectra of five isotopic species of the CH_3Cl−HCl hydrogen bond complex as well as the IR spectra in the H(D)−Cl stretching mode region at 196 K and under jet-cooled conditions.

Theoretically, the CCSD(T) level is necessary to achieve sufficient accuracy in both the structure and the frequencies for this type of hydrogen-bond complex. If the CBS extrapolation tends to give a better agreement with experiment, the deviations from the results obtained with the AVQZ basis set are very low and are lost in the approximations made for the treatment of anharmonicity (both on the frequencies and on the ground state geometry). For the study of similar systems, the CCSD(T)/AVQZ level of theory should be sufficient if there is no improvement in the anharmonicity treatment.

As already shown for other hydrogen bond complexes, a strong coupling scheme between the H−Cl stretching and the intermolecular modes is observed. However, in the present case, the complementary experimental and theoretical results tend to reveal a free rotation of the CH_3Cl unit. It is pointing out the very peculiar dynamical properties of a hydrogen bond and, consequently, the necessity of taking those effects into account to correctly model the intra- and intermolecular interactions.

■ ASSOCIATED CONTENT

Ⓢ Supporting Information

Rotational line assignments, measured frequencies, experimental uncertainties and deviations from the final fits for the six studied isotopes in the MW region. This material is available free of charge via the Internet at http://pubs.acs.org.

■ AUTHOR INFORMATION

Corresponding Author

*M. Goubet. Telephone: +33-3-20434905. Fax: +33-3-20337020. E-mail: manuel.goubet@univ-lille1.fr.

Notes

The authors declare no competing financial interest.

■ ACKNOWLEDGMENTS

The authors are indebted to Prof. T. H. Huet for numerous discussions and very helpful comments on this work.

■ REFERENCES

(1) Aakeröy, C. B.; Seddon, K. R. The Hydrogen Bond and Crystal Engineering. *Chem. Soc. Rev.* **1993**, *22*, 397−407.
(2) Puru, J.; Castleman, A. W., Jr. Clusters: A Bridge Across the Disciplines of Physics and Chemistry. *Proc. Natl. Acad. Soc. U. S. A.* **2006**, *103*, 10560−10569.
(3) Trotman-Dickenson, A. *Comprehensive Inorganic Chemistry*; Pergamon Press: Oxford, U.K., 1973.
(4) Ingold, C. K. *Structure and Mechanism in Organic Chemistry*, 2nd ed.; Cornell University Press: Ithaca, NY, 1969.
(5) Klemperer, W.; Vaida, V. Molecular Complexes in Close and Far Away. *Proc. Natl. Acad. Soc. U. S. A.* **2006**, *103*, 10584−10588.
(6) Jeffrey, G. A.; Saenger, W. *Hydrogen Bonding in Biological Structures*; Springer: Berlin, 1991.
(7) Desiraju, G. R.; Steiner, T. *The Weak Hydrogen Bond in Structural Chemistry and Biology*; Oxford University Press: New York, 1999.
(8) See, e.g.: Structure and Dynamics of Van der Waals Complexes. *Faraday Discuss.* **1994**, *97*.
(9) See, e.g., special issue: Spectroscopic probes for molecular recognition. *Phys. Chem. Chem. Phys.* **2007**, *9*, 4429−4608.
(10) Cézard, C.; Rice, C. A.; Shum, M. A. OH-Stretching Red Shifts in Bulky Hydrogen-Bonded Alcohols: Jet Spectroscopy and Modeling. *J. Phys Chem. A* **2006**, *110*, 9839−9848.
(11) McKerell, A. D., Jr. Empirical Force Fields for Biological Macromolecules: Overview and Issues. *J. Comput. Chem.* **2004**, *25*, 1584−1604.
(12) Weber, A. *Structure and Dynamics of Weakly Bound Molecular Complexes*; NATO ASI series: Series C, Mathematical and physical sciences, Vol. *212*; Springer: Berlin, 1986.
(13) Nesbitt, D. J. High-resolution Infrared Spectroscopy of Weakly Bound Molecular Complexes. *Chem. Rev.* **1988**, *88*, 843−870.
(14) Leopold, K. R.; Fraser, G. T.; Novick, S. E.; Klemperer, W. Current Themes in Microwave and Infrared Spectroscopy of Weakly Bound Complexes. *Chem. Rev.* **1994**, *94*, 1807−1827.
(15) Legon, A. C. Prereactive Complexes of Dihalogens XY with Lewis Bases B in the Gas Phase: A Systematic Case for the Halogen Analogue B···XY of the Hydrogen Bond B···HX. *Angew. Chem., Int. Ed.* **1999**, *38*, 2686−2714.
(16) Miller, R. E. Spiers Memorial Lecture. Comparative Studies of Cluster Dynamics in the Gas and Condensed Phases. *Faraday Discuss.* **2001**, *118*, 1−18.
(17) Keutsch, F. N.; Saykally, R. J. Water Clusters: Untangling the Mysteries of the Liquid, One Molecule at a Time. *Proc. Natl. Acad. Soc. U. S. A.* **2001**, *98*, 10533−10540.
(18) Klopper, W.; Quack, M.; Suhm, M. A. A New Ab Initio Based Six-Dimensional Semi-Empirical Pair Interaction Potential for HF. *Chem. Phys. Lett.* **1996**, *261*, 35−44.
(19) Fellers, R. S.; Braly, L. B.; Saykally, R. J.; Leforestier, C. Fully Coupled Six-Dimensional Calculations of the Water Dimer Vibration-Rotation-Tunneling States with Split Wigner Pseudospectral Approach. II. Improvements and Tests of Additional Potentials. *J. Chem. Phys.* **1999**, *110*, 6306−6318.
(20) Nesbitt, D. J.; Field, R. W. Vibrational Energy Flow in Highly Excited Molecules: Role of Intramolecular Vibrational Redistribution. *J. Phys. Chem.* **1996**, *100*, 12735−12756.
(21) Millen, D. J. Vibrational Spectra and Vibrational States of Simple Gas-Phase Hydrogen-Bonded Dimers. *J. Mol. Struct.* **1983**, *100*, 351−377.
(22) Legon, A. C. Non-Linear Hydrogen Bonds and Rotational Spectroscopy: Measurement and Rationalisation of the Deviation from Linearity. *Faraday Discuss.* **1994**, *97*, 19−33.
(23) Antolinez, S.; Lopez, J. C.; Alonso, J. L. The Axial and Equatorial Hydrogen Bonds in the Tetrahydropyran···HF Complex. *Chem. Phys. Chem.* **2001**, *2*, 114−117.
(24) Ault, B. S.; Balboa, A.; Tevault, D.; Hurley, M. Matrix Isolation Infrared Spectroscopic and Theoretical Study of the Interaction of Water with Dimethyl Methylphosphonate. *J. Phys. Chem. A* **2004**, *108*, 10094−10098.
(25) Barnes, A. J. Matrix Isolation Infrared Spectroscopic and Theoretical Study of the Interaction of Water with Dimethyl Methylphosphonate. *J. Mol. Struct.* **1983**, *100*, 259−280.
(26) Perchard, J. P.; Mielke, Z. Anharmonicity and Hydrogen bonding: I. A Near-Infrared Study of Methanol Trapped in Nitrogen and Argon Matrices. *Chem. Phys.* **2001**, *264*, 221−234.
(27) Asselin, P.; Dupuis, B.; Perchard, J. P.; Soulard, P. The Gas Phase Infrared Spectrum of HCl Complexed with Dimethyl Ether Revisited: Assignment of the Fundamental Transition from a Jet-Cooled Experiment. *Chem. Phys. Lett.* **1997**, *268*, 265−272.
(28) Häber, T.; Schmitt, U.; Suhm, M. A. FTIR-Spectroscopy of Molecular Clusters in Pulsed Supersonic Slit-Jet Expansions. *Phys. Chem. Chem. Phys.* **1999**, *1*, 5573−5582.
(29) Cirtog, M.; Asselin, P.; Soulard, P.; Tremblay, B.; Madebène, B.; Alikhani, M. E.; Georges, R.; Moudens, A.; Goubet, M.; Huet, T. R.; et al. The $(CH_2)_2O$−H_2O Hydrogen Bonded Complex. Ab Initio Calculations and Fourier Transform Infrared Spectroscopy from Neon Matrix and a New Supersonic Jet Experiment Coupled to the Infrared AILES Beamline of Synchrotron SOLEIL. *J. Phys. Chem. A* **2011**, *115*, 2523−2532.

(30) Suhm, M. A.; Kollipost, F. Femtisecond Single-Mole Infrared Spectroscopy of Molecular Clusters. *Phys. Chem. Chem. Phys.* **2013**, *15*, 10702−10721.
(31) Kassi, S.; Petitprez, D.; Wlodarczak, G. Microwave Fourier Transform Spectroscopy of t-Butylchloride and t-Butylbromide Isotopic Species. *J. Mol. Struct.* **2000**, *517/518*, 375−386.
(32) Asselin, P.; Soulard, P.; Tarrago, G.; Lacome, N.; Manceron, L. High Resolution Fourier Transform Infrared Spectroscopy of the ν_6 and ν_{10} Bands of Jet-Cooled $Fe(CO)_5$. *J. Chem. Phys.* **1996**, *104*, 4427−4433.
(33) Asselin, P.; Soulard, P.; Alikhani, M. E.; Perchard, J. P. A New Interpretation of the IR Spectrum of H(D)Cl Complexed with Dimethyl Ether from a Supersonic Jet-FTIR Experiment. *Chem. Phys.* **1999**, *249*, 73−87.
(34) Frisch, M. J.; et al. *Gaussian 09*, Revision A.02; Gaussian, Inc.: Wallingford, CT, 2009.
(35) Werner, H.-J.; Knowles, P. J. *MOLPRO, a package of ab initio programs*; Cardiff University: Cardiff, U.K., 2012.
(36) Dunning, T. H., Jr. Gaussian Basis Sets for Use in Correlated Molecular Calculations. I. The Atoms Boron Through Neon and Hydrogen. *J. Chem. Phys.* **1989**, *90*, 1007−1023.
(37) Woon, D. E.; Dunning, T. H., Jr. Gaussian Basis Sets for Use in Correlated Molecular Calculations. III. The Atoms Aluminum through Argon. *J. Chem. Phys.* **1993**, *98*, 1358−1371.
(38) Kendall, R. A.; Dunning, T. H., Jr.; Harrison, R. J. Electron Affinities of the First Row Atoms Revisited. Systematic Basis Sets and Wave Functions. *J. Chem. Phys.* **1992**, *96*, 6796−6806.
(39) Peterson, K. A.; Woon, D. E.; Dunning, T. H., Jr. Benchmark Calculations with Correlated Molecular Wave Functions. IV. The Classical Barrier Height of the $H+H_2 \rightarrow H_2+H$ Reaction. *J. Chem. Phys.* **1994**, *100*, 7410−7415.
(40) Woon, D. E.; Dunning, T. H., Jr. Benchmark Calculations with Correlated Molecular Wave Functions. VI. Second Row A_2 and First Row/Second Row AB Diatomic Molecules. *J. Chem. Phys.* **1994**, *101*, 8877−8893.
(41) Barone, V. Anharmonic vibrational properties by a fully automated second-order perturbative approach. *J. Chem. Phys.* **2005**, *122*, 14108−14118.
(42) Martson, C. C.; Balin-Kurti, G. G. The Fourier Grid Hamiltonian Method for Bound State Eigenvalues and Eigenfunctions. *J. Chem. Phys.* **1989**, *91*, 3571−3576.
(43) Balin-Kurti, G. G.; Ward, C. L.; Martson, C. C. Two Computer Programs for Solving the Schrödinger Equation for Bound-State Eigenvalues and Eigenfunctions Using the Fourier Grid Hamiltonian Method. *Comput. Phys. Commun.* **1991**, *67*, 285−292.
(44) Kraitchman, J. Determination of Molecular Structure from Microwave Spectroscopic Data. *Am. J. Phys.* **1953**, *21*, 17−24.
(45) Pickett, H. M. The Fitting and Prediction of Vibration-Rotation Spectra with Spin Interactions. *J. Mol. Spectrosc.* **1991**, *148*, 371−377. See also http://spec.jpl.nasa.gov.
(46) Gordy, W.; Cook, R. L. *Microwave molecular spectra*, 3rd ed.; John Wiley & Sons, Inc.: New York, 1984.
(47) Kraitchman, J.; Dailey, B. P. Variation in the Quadrupole Coupling Constant with Vibrational State in the Methyl Halides. *J. Chem. Phys.* **1954**, *22*, 1477−1481.
(48) De Lucia, F. C.; Helminger, P.; Gordy, W. Submillimeter-Wave Spectra and Equilibrium Structures of the Hydrogen Halides. *Phys. Rev. A* **1971**, *3*, 1849−1857.
(49) Asselin, P.; Goubet, M.; Lewerenz, M.; Soulard, P.; Perchard, J. P. Rovibrational and Dynamical Properties of the Hydrogen Bonded Complex $(CH_2)_2$S-HF: A Combined Free Jet, Cell, and Neon Matrix-Fourier Transform Infrared Study. *J. Chem. Phys.* **2004**, *121*, 5241−5252.
(50) Asselin, P.; Goubet, M.; Latajka, Z.; Soulard, P.; Lewerenz, M. Vibrational Dynamics of the Hydrogen Bonded Complexes $(CH_2)_2$O−HF and −DF Investigated by Combined Jet- and Cell-Fourier Transform Infrared Spectroscopy. *Phys. Chem. Chem. Phys.* **2005**, *7*, 592−599.
(51) Duncan, J. L.; Law, M. M. A Study of Vibrational Anharmonicity, Fermi Resonance Interactions, and Local Mode Behavior in CH_3Cl. *J. Mol. Spectrosc.* **1990**, *140*, 13−30.
(52) Huber, K. P.; Herzberg, G. *Molecular Spectra and Molecular Structure. IV Constants of Diatomic Molecules*; Van Nostrand Reinhhold Co.: New York, 1979.
(53) Herrebout, W. A.; Van der Veken, B. J. Infrared Spectra, Relative Stability, and Ab Initio Calculations of the Methyl-d3 Chloride-Hydrogen Chloride Van der Waals Complex Observed in Liquefied Argon. *J. Phys. Chem.* **1993**, *97*, 10622−10629.
(54) Herrebout, W. A.; Van der Veken, B. J.; Durig, J. R. On the Angular Geometry of the $CH_3Cl \cdot HCl$ Van der Waals Complex in the Gas Phase and in Liquefied Noble Gas Solutions. *J. Mol. Struct.* **1995**, *332*, 231−240.
(55) Duncan, J. L.; McKean, D. C.; Mallinson, P. D.; McCulloch, R. D. Infrared Spectra of CHD_2Cl and CHD_2CCH and the Geometries of Methyl Chloride and Propyne. *J. Mol. Spectrosc.* **1973**, *46*, 232−239.
(56) Jensen, P.; Bordensen, S.; Gualachvili, G. Determination of A_0 for $CH_3{}^{35}Cl$ and $CH_3{}^{37}Cl$ from the ν_4 Infrared and Raman Bands. *J. Mol. Spectrosc.* **1981**, *88*, 378−393.
(57) Hujo, W.; Grimme, S. Comparison of the Performance of Dispersion-Corrected Density Functional Theory for Weak Hydrogen Bonds. *Phys. Chem. Chem. Phys.* **2011**, *13*, 13942−13950.
(58) Goubet, M.; Asselin, P.; Soulard, P.; Lewerenz, M.; Latajka, Z. Vibrational Dynamics of Medium Strength Hydrogen Bonds: Fourier Transform Infrared Spectra and Band Contour Analysis of the DF Stretching Region of $(CH_2)_2$S−DF. *J. Chem. Phys.* **2004**, *121*, 7784−7794.
(59) Costain, C. C. Determination of Molecular Structures from Ground State Rotational Constants. *J. Chem. Phys.* **1958**, *29*, 864−874.
(60) Demaison, J. Experimental, Semi-Experimental and Ab Initio Equilibrium Structures. *Mol. Phys.* **2007**, *105*, 3109−3138.
(61) Tang, S.; Majerz, I.; Caminati, W. Sizing the Ubbelohde effect: the rotational spectrum of a tert-butyalcohol dimer. *Phys. Chem. Chem. Phys.* **2011**, *13*, 9137−9139 and references therein.
(62) Asselin, P.; Soulard, P.; Madebène, B.; Alikhani, M. E.; Lewerenz, M. Vibrational Dynamics of the Hydrogen Bond in H_2S−HF: Fourier-Transform-Infrared Spectra and Ab Initio Theory. *Phys. Chem. Chem. Phys.* **2006**, *8*, 1785−1793.
(63) Asselin, P.; Soulard, P.; Madebène, B.; Lewerenz, M. Fourier Transform Infrared Spectroscopy and Ab Initio Theory of Acid−Hydrogen Sulfide Clusters: H_2S−HCl, D_2S−DCl and $H_2S-(HCl)_2$. *Phys. Chem. Chem. Phys.* **2007**, *9*, 2868−2876.
(64) Goubet, M.; Madebène, B.; Lewerenz, M. Coupled Anharmonic Vibrational Dynamics of the Hydrogen Bond in Binary Complexes. *Chimia* **2004**, *58*, 291−295.
(65) Madebène, B. *Ph.D. Thesis*, Université Pierre et Marie Curie Paris VI, Paris, 2005
(66) Caminati, W.; Lopez, J. C.; Alonso, J. L.; Grabow, J.-U.; Weak, CH—F Bridges and Internal Dynamics in the CH_3F-CHF_3 Molecular Complex. *Angew. Chem., Int. Ed.* **2005**, *44*, 3840−3844.
(67) Herschbach, D. R. Calculation of Energy Levels for Internal Torsion and OverAll Rotation. III. *J. Chem. Phys.* **1959**, *31*, 91−108.